Steel and Composite Structures, *Vol. 36, No. 3 (2020) 273-291*
DOI: https://doi.org/10.12989/scs.2020.36.3.273

Seismic design rules for ductile Eurocode-compliant two-storey X concentrically braced frames

Silvia Costanzo[a], Mario D'Aniello* and Raffaele Landolfo[b]

Department of Structures for Engineering and Architecture, University of Naples "Federico II", Via Forno Vecchio 36, 80134 Naples, Italy

(*Received January 21, 2020, Revised June 29, 2020, Accepted July 5, 2020*)

Abstract. Two-storey X-bracings are currently very popular in European practice, as respect to chevron and simple X bracings, owing to the advantages of reducing the bending demand in the brace-intercepted beams in V and inverted-V configurations and optimizing the design of gusset plate connections. However, rules for two-storey X braced frames are not clearly specified within current version of EN1998-1, thus leading to different interpretations of the code by designers. The research presented in this paper is addressed at investigating the seismic behaviour of two-storey X concentrically braced frames in order to revise the design rules within EN1998-1. Therefore, five different design criteria are discussed, and their effectiveness is investigated. With this aim, a comprehensive numerical parametric study is carried out considering a set of planar frames extracted from a set of structural archetypes that are representative of regular low, medium and high-rise buildings. The obtained results show that the proposed design criteria ensure satisfactory seismic performance.

Keywords: concentrically braced frames; two-storey CBF, eurocode 8; capacity design; bracings; seismic design

1. Introduction

Two-storey X concentrically braced frames (also called split-X CBFs) are often opted by structural engineers in seismic design of steel buildings. Two-storey X configuration is obtained by using V and inverted V bracings for two consecutive storeys (see Fig. 1), with the aim to reduce the bending demand typically observed in the brace-intercepted beam of V and inverted-V configurations (Shen *et al.* 2014, 2015). Indeed, the forces occurring in the post-buckling range below and above the beam are in opposite direction (see Fig. 2(a)), thus limiting the bending and axial actions on the beam. In addition, arranging bracings as shown in Fig. 1(c) allows overcoming geometrical and technological difficulties commonly recognized in the design of traditional X braced frames (Silva *et al.* 2019).

As shown in Fig. 3, for typical values of storey height and span length used in common European steel structural buildings, using diagonal members in simple X configurations may entail impractical brace-to-beam angles (e.g., either smaller than 30° or larger than 60°), resulting in quite large and expensive gusset connections at brace-to-beam/column intersections. Conversely, the chevron and the two-storey X configurations generally allow suitable slope of diagonal members, i.e., in the range [30°-60°] (Astaneh-Asl *et al.* 2006, Silva *et al.* 2019), for efficient design of gusset plate connections (see Fig. 3).

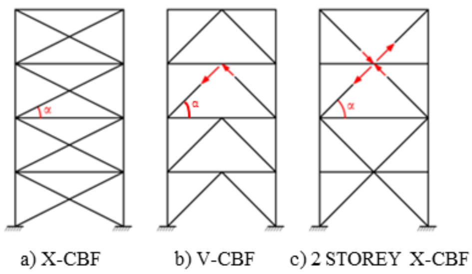

Fig. 1 Typical configurations of CBFs

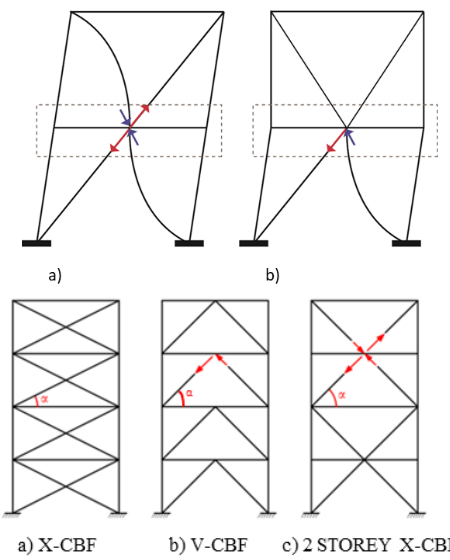

Fig. 2 Plastic mechanisms and loading patterns: (a) uniform yielding and (b) soft-storey mechanism

*Corresponding author, Associate Professor
E-mail: mdaniel@unina.it
[a]Ph.D.
[b]Professor

http://www.techno-press.org/?journal=scs&subpage=8
ISSN: 1229-9367 (Print), 1598-6233 (Online)

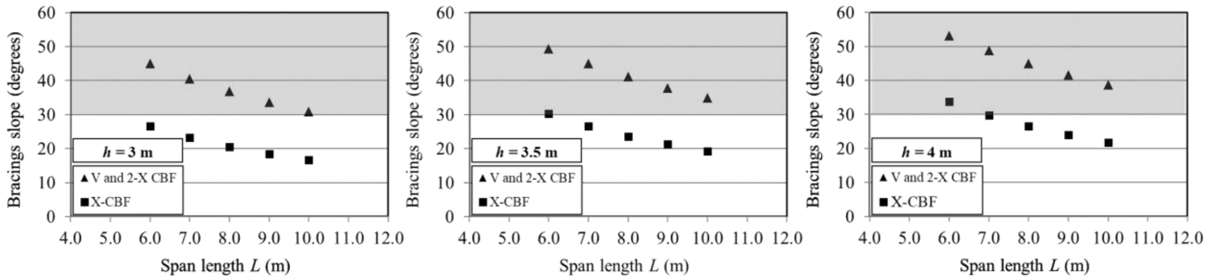

Fig. 3 Slope of concentrically bracings in X, V or two-storey X configurations

Even though two-storey X-bracings are very attractive for practitioner engineers, the design rules of current EN1998-1 (hereinafter also indicated as EC8 or Eurocode 8) for this system are not clearly detailed, thus leading to different interpretations of the code by designers. Indeed, on the basis of the experience matured by the Authors within several training courses for structural engineers held across Europe, a large number of designers consider two-storey X-bracings in the same manner of simple X bracings, namely to be designed considering only the tension diagonals as active (TO model) and disregarding their post-buckling behaviour.

On the contrary, other designers adopt the same rule of V bracings, namely considering as active both tension and compression diagonals in the structural model (TC model). In the opinion of the Authors, the possibility of different interpretations of the code is critical and potentially unsafe. These considerations motivated the study summarized hereinafter, which was carried out within the activities of ECCS TC13 and WG2/CEN/TC250 committees, devoted to revise the criticisms of EN1998-1 design rules for steel and steel-composite structures.

The main objectives of the research presented in the current paper are the following:

(i) To evaluate the main structural parameters affecting the seismic performance of two-storey X concentrically braced frames.

(ii) To assess and compare the effectiveness of design provisions currently codified in European and US seismic standards.

(iii) To propose new rules for ductile two-storey X CBF as possible amendment of next EC8.

To achieve these aims, a numerical parametric study based on nonlinear dynamic analyses was carried out on a set of reference buildings alternatively designed according to different design criteria. The comparison of the obtained results clearly highlights which is the more effective criterion for possible amendment of EN 1998-1 to enhance the overall ductility of two-storey X CBFs.

2. North american vs European design rules

The capacity design criteria provided by current seismic codes for ductile concentrically braced frames (e.g., DCH concept in EN1998-1, Special CBFs in AISC341-16) theoretically aim at guaranteeing the yielding of diagonal members and preserving the connected beams and columns from damage. Both European and North-American codes for V and inverted-V types recommend calculating the bending moment acting on the beams connected to the diagonals by performing a plastic mechanism analysis in which the braces are assumed yielded under tension and buckled under compression. AISC341-16 extends this approach to the two-storey X configuration (as also shown in AISC Design Manual 2018) and it is implicitly based on the assumptions that global plastic mechanism develops and the braces at two consecutive storeys reach the same level of plastic deformation (see Fig. 2(a)). However, the storey drift ratios of two consecutive storeys are generally different, as well as the loading patterns applied at the brace-intercepted beams (Shen *et al.* 2014, 2015). If soft-storey mechanism occurs, the braces above and below the beam experience different level of deformation and the drift ratios at the two consecutive storeys could be significantly different. In this scenario, the pattern of forces applied on brace-intercepted beams tend to that typically observed in chevron CBFs, namely a large unbalanced force is applied at the beam mid-length (see Fig. 2(b)).

Previous studies (Khatib *et al.* 1998, Chen and Mahin 2012, Yoo *et al.* 2009, Hsiao *et al.* 2013) addressed the overall seismic behaviour of two-storey X-CBFs, but not specifically focused on the design rules for the beam connected to the diagonals. More recently, Shen *et al.* (2014, 2015, 2017) investigated the key role of the brace-intercepted beam in both V and inverted V and in two-storey X concentrically braced frames. In these studies, the seismic response of two-storey X concentrically braced frames is discussed in terms of seismic strength and deformation demand on beams, to determine whether flexural yielding occurs at brace-intercepted section. Results from numerical analyses show that beams designed according to current US provisions (AISC341-16) would experience significant vertical deflection and the formation of plastic hinges at storey drift ratios of about 0.02 rad (Shen *et al.* 2014). Flexural yielding of the brace-intercepted beam may cause significant loss of strength and stiffness and very poor energy dissipation capacity if compared to the expected performance of special braced frames (Shen *et al.* 2014, 2015). Further studies on chevron concentrically braced frames (D'Aniello *et al.* 2015a, Costanzo *et al.* 2016,2017a, b) confirm that current design provisions can be less effective in assuring global ductile mechanism, because the codes solely focus on the beam strength. As suggested by D'Aniello *et al.* (2015a), the flexural stiffness of the brace-intercepted beam is a key parameter to be controlled to guarantee the brace yielding in tension and to avoid large vertical deflection of the beam. Indeed, significant vertical deflection of the beam can prevent the yielding of brace under tension and impose severe ductility demand under compression. On the other hand, as observed by Uriz and Mahin (2008) deep girders might impose significant flexural demand on beam-to-column connections, likely inducing plastic hinge in the columns or premature fracture of the beam-to-column connections.

Owing to the low redundancy of concentrically braced frames, these systems are likely prone to soft-storey mechanisms, with concentration of large ductility demand after the yielding of diagonal members is reached at the soft storey (Costanzo *et al.* 2017b, Elghazouli 2010, Costanzo and Landolfo 2017). To mitigate this feature and to promote more uniform distribution of plastic deformations along the building height, EN 1998-1 limits the capacity-to-demand ratio of diagonal members $\Omega_i = N_{pl,br,Rd,i}/N_{Ed,br,i}$, which should not vary more than the 25%. Several Authors (Costanzo *et al.* 2017b,2018, 2019, Silva *et al.* 2018, Marino 2013, Bosco *et al.* 2017, Barbagallo *et al.* 2019, Longo *et al.* 2008, 2015, 2016, Metelli 2013) underlined that such requirement is not effective in assuring uniform distribution of plastic deformation along the building eight, and it imposes additional design efforts and practical difficulties in sizing of diagonals (Costanzo *et al.* 2017b, 2018, 2019, Silva *et al.* 2018, Marino 2013). With this regard, Costanzo *et al.* (2017b, 2019) recognized that using a compression-based approach to define the capacity-to-demand ratio (namely considering the compression axial strength of bracings in place of the plastic capacity) can be more effective to inhibit the activation of soft-storey mechanisms. This approach bases on the fact that the buckling of the brace under compression is the first nonlinear event occurring at each storey, and thus it allows better controlling the sequence of braces buckling along the building height and the displacement shape profile. Differently from EN 1998-1, North American codes (i.e., AISC341-16 and CSA-S16) do not require any control of capacity-to-demand ratio at each storey along the building height. However, it is common practice to use fully restrained moment beam-to-column joints into the braced bays of Special Concentrically Braced Frames (SCBFs) that implicitly introduce redundancy and it is beneficial to improve the redistribution of damage along the building height.

To mitigate the possibility of activation of soft-storey mechanisms, several Authors (e.g., Khatib *et al.* 1988, Tremblay *et al.* 2003, Wijesundara *et al.* 2018) proposed adding a zipper strut to the V or inverted V configuration between the brace-intercepted section and the mid-span of the floor beam, to transmit the vertical force occurring in the brace post-buckling range to the storeys above. Even though the zipper configuration demonstrated to be efficient in achieving uniform distribution of plastic deformation along the building height, it is not very attractive due to architectural limitations (e.g., the difficulties in placing openings).

Further aspect deserving to be discussed concerns the design of columns belonging to the braced bays. After the braces yield in tension, the interstorey drift demand typically increases, leading to additional bending demand on the columns. The simultaneous action of axial force and bending demand in the columns of the braced bays is not directly accounted for by both US and European codes, thus leading to potential detrimental effects on the global stability of the braced frame. Conversely, according to CSA-S16 the stability of the braced column should be checked against the combined action of the axial force (evaluated by mean of plastic-mechanism analysis) and a bending moment in the direction of the braced bay equal to the 20% of the plastic flexural capacity of the column cross section.

3. Parametric study

Five different design criteria were investigated and validated by mean of nonlinear dynamic analyses carried out on low, medium and high-rise residential buildings equipped with two-storey X bracings. It is worth noting that some of these criteria are mainly derived from the discussions inferred with several designers (see criteria 1, 2 and 3 in the next sections). Therefore, they can be considered as representative of current European practice.

The design rules are varied with specific reference to the most critical issues mentioned in Section 2, namely:

(i) Design of diagonal bracings: the influence of using tension-only (TO) model (in which the presence of compression diagonals is disregarded) rather than tension-compression one (TC) to perform global elastic analysis is investigated; the rules for homogeneity condition of capacity-to-demand ratio and the brace slenderness limitation are also varied.

(ii) Design of brace-intercepted beam: different loading scenarios are considered, and capacity design rules are consistently varied.

(iii) Design of columns: capacity design rules and influence of combined axial forces and bending moments are investigated.

3.1 Design criteria

3.1.1 Criterion 1

The first design criterion (C1) assumes that, in absence of specific provisions, European engineers may design two-storey X-CBFs consistently to conventional cross bracings. Thereby, the seismic design provisions currently codified in EN1998-1 for X-CBFs are extended to the two-storey X configuration, as summarized in the following:

- The seismic-induced effects on diagonal members are evaluated by performing a linear-elastic analysis on a tension-only (TO) diagonals scheme, where the compression diagonals are omitted in. (See row C1 in Fig. 4). The bracings are designed to guarantee $N_{pl,br,Rd} \geq N_{Ed,br}$, where $N_{pl,br,Rd}$ is the design plastic strength of brace cross-section and $N_{Ed,br}$ is calculated according to the TO scheme shown in Fig. 4 - row C1.

		Design of bracings	Design of beams	Design of columns
C1	TO model 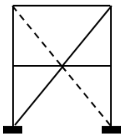	**Required strength:** $N_{Ed,br,i} \le N_{pl,br,Rd,i}$ **Normalized slenderness limits:** $1.3 \le \bar{\lambda} \le 2$ **Storey-to-storey distribution of tension overstrength ratios:** $\Omega_i = \frac{N_{pl,br,Rd,i}}{N_{Ed,br,i}}$ $\left[(\Omega_i - \Omega)/\Omega\right] \le 0.25\ ,\ i \in [1,n]$	**Required strength:** **(elastic analysis)** $N_{pl,Rd,i}(M_{Ed}) \ge N_{Ed,G,i} + 1.1 \cdot \gamma_{ov} \cdot \Omega \cdot N_{Ed,1}$	**Required strength:** **(elastic analysis)** $N_{pl,Rd,i}(M_{Ed}) \ge N_{Ed,G,i} + 1.1 \cdot \gamma_{ov} \cdot \Omega \cdot N_{Ed,E,i}$
C2	TC model 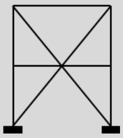	**Required strength:** $N_{Ed,br,i} \le \chi N_{pl,br,Rd,i}$ **Normalized slenderness limit:** $\bar{\lambda} \le 2$ **Storey-to-storey distribution of tension overstrength ratios:** $\Omega_i = \frac{N_{pl,br,Rd,i}}{N_{Ed,br,i}}$ $\left[(\Omega_i - \Omega)/\Omega\right] \le 0.25\ ,\ i \in [1,n]$	**Required strength:** **(plastic mechanism analysis)** 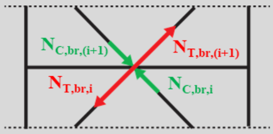 $N_{C,br,i} = 0.3 N_{pl,br,Rd,i}$ $N_{T,br,i} = N_{pl,br,Rd,i}$	**Required strength:** **(plastic mechanism analysis)** 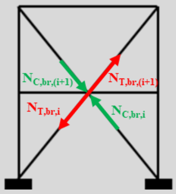 $N_{C,br,i} = 0.3 N_{pl,br,Rd,i}$ $N_{T,br,i} = N_{pl,br,Rd,i}$
C3	TC model 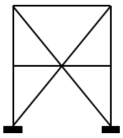	**Required strength:** $N_{Ed,br,i} \le \chi N_{pl,br,Rd,i}$ **Normalized slenderness limit:** $\bar{\lambda} \le 2$ **Storey-to-storey distribution of tension overstrength ratios:** $\Omega_i = \frac{N_{pl,br,Rd,i}}{N_{Ed,br,i}}$ $\left[(\Omega_i - \Omega)/\Omega\right] \le 0.25\ ,\ i \in [1,n]$	**Required strength:** **(plastic mechanism analysis)** 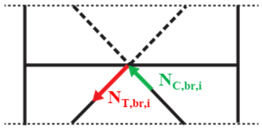 $N_{C,br,i} = 0.3 \cdot N_{pl,br,Rd,i}$ $N_{T,br,i} = N_{pl,br,Rd,i}$	**Required strength:** **(plastic mechanism analysis)** 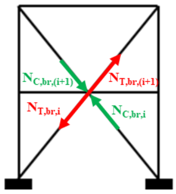 $N_{C,br,i} = 0.3 N_{pl,br,Rd,i}$ $N_{T,br,i} = N_{pl,br,Rd,i}$
C4	TC model 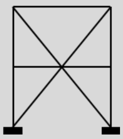	**Required strength:** $N_{Ed,br,i} \le \gamma_{ov} \cdot \chi \cdot N_{pl,br,Rd,i}$ **Geometrical slenderness limit:** $\frac{KL}{r} \le 200$ **Storey-to-storey distribution of tension overstrength ratios:** NO	**Required strength:** **(plastic mechanism analysis)** 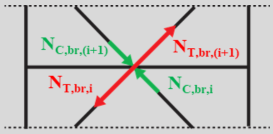 **The most severe condition between pre-buckling situation:** $N_{T,br,i} = N_{C,br,i} = \chi \cdot \gamma_{ov} \cdot N_{pl,br,Rd,i}$ **and post-buckling situation:** $N_{C,br,i} = 0.3 \cdot \chi \cdot \gamma_{ov} \cdot N_{pl,br,Rd,i}$ $N_{T,br,i} = \gamma_{ov} \cdot N_{pl,br,Rd,i}$	**Required strength:** **Maxima seismic-induced effects evaluated by:** **(1) elastic analysis with amplification factor Ω_o=2;** 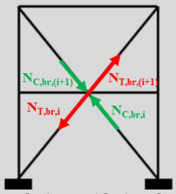 **(2) plastic analysis considering the most severe condition between pre-buckling situation:** $N_{T,br,i} = N_{C,br,i} = \chi \cdot \gamma_{ov} \cdot N_{pl,br,Rd,i}$ **and post-buckling situation:** $N_{C,br,i} = 0.3 \cdot \chi \cdot \gamma_{ov} \cdot N_{pl,br,Rd,i}$ $N_{T,br,i} = \gamma_{ov} \cdot N_{pl,br,Rd,i}$
C5	TC model 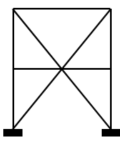	**Required strength:** $N_{Ed,br} \le \chi N_{pl,br,Rd}$ **Normalized slenderness limit:** $\bar{\lambda} \le 2$ **Storey-to-storey distribution of buckling overstrength ratios:** $\Omega_{b,i} = \frac{\chi \cdot N_{pl,br,Rd,i}}{N_{Ed,br,i}}$ $\left[(\Omega_{b,i} - \Omega_b)/\Omega_b\right] \le 0.25\ ;\ i \in [1,n-1]$	**Required strength:** **(plastic mechanism analysis)** **The most severe condition between:** 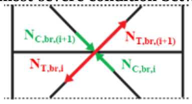 **and** 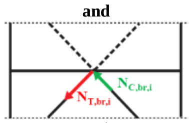 **assuming:** $N_{C,br,i} = 0.3 \cdot \chi \cdot \gamma_{ov} \cdot N_{pl,br,Rd,i}$ $N_{T,br,i} = 1.1 \cdot \gamma_{ov} \cdot N_{pl,br,Rd,i}$	**Required strength:** **Axial forces by plastic mechanism analysis** 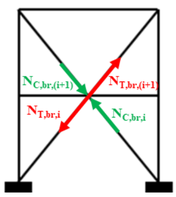 $N_{C,br,i} = 0.3 \cdot \chi \cdot \gamma_{ov} \cdot N_{pl,br,Rd,i}$ $N_{T,br,i} = 1.1 \cdot \gamma_{ov} \cdot N_{pl,br,Rd,i}$ **and** **uniform bending moment in the columns** $M_{Ed,E,i} = 0.2 \cdot M_{pl,i}$

Fig. 4 Synoptic overview of the examined design criteria

- The brace normalized slenderness $\bar{\lambda}$ varies within the range [1.3, 2] (EN 1998-1 6.7.3(1)).
- The tension overstrength ratio $\Omega_i = N_{pl,br,Rd,i}/N_{Ed,br,i}$ satisfies the condition $[(\Omega_i - \Omega)/\Omega] \leq 0.25$, with $\Omega = \min(\Omega_i)$ and $i \in [1,n]$, being n the number of storeys.
- The brace-intercepted beam is verified against combined axial force and bending moment due to the difference between the elastic tensile forces in the braces above and below the beam that are calculated with TO model.
- The required strength of columns is evaluated by adding to the effects due to the gravity loads those obtained from seismic forces, the latter magnified by the minimum brace overstrength ratio Ω, as follows

$$N_{Rd}(M_{Ed}) \geq N_{Ed,G} + 1.1 \cdot \gamma_{ov} \cdot \Omega \cdot N_{Ed,E} \quad (1)$$

where:

$N_{Rd}(M_{Ed})$ is the design axial resistance of the members calculated in accordance with EN 1993:1-1, taking into account the interaction with the design value of bending moment, M_{Ed}, in the seismic design situation; $N_{Ed,G}$ is the axial force in the non-dissipative member due to the gravity loads included in the combination of actions for the seismic design situation;

$N_{Ed,E}$ is the axial force induced by the seismic event;

γ_{ov} is the material randomness coefficient;

Ω is the minimum overstrength ratio $\Omega_i = N_{pl,bRd,i}/N_{Ed,br,i}$.

3.1.2 Criterion 2

In the second design criterion (C2) the structures are designed by applying contemporarily EN1998-1 design rules for V and inverted V concentric bracings to two consecutive storeys, as follows:

- The internal forces acting on the bracings are evaluated by performing global elastic analysis on a tension-compression (TC) model. Therefore, the bracings at the i-th storey verify $N_{b,br,Rd,i} \geq N_{Ed,br,i}$ where $N_{b,br,Rd,i}$ is the design buckling strength of brace cross-section and $N_{Ed,br,i}$ is calculated according to the TC scheme.
- The braces normalized slenderness are limited to $\bar{\lambda} \leq 2$.
- The control of tension overstrength ratio is kept as in C1.
- The seismic-induced effects on non-dissipative members (i.e., beams and columns) are evaluated by performing a plastic mechanism analysis, in which both V and inverted V bracings above and below the beam are assumed to reach their ultimate resistance, namely the plastic strength $N_{pl,br,Rd,i}$ in the braces under tension and the post-buckling capacity $0.3N_{pl,br,Rd,i}$ in those under compression, in accordance with EN1998-1. It is worth mentioning that slender bracings, even within the upper bound limit 2, exhibit buckling capacity generally about 0.2 times the relevant plastic strength, namely smaller than the residual compression capacity evaluated according to EN1998-1.
- The beam connected to diagonal members is designed for the contemporary presence of axial and shear forces and bending moment, considering: (i) non-seismic (gravity) loads without accounting for the intermediate support given by the bracings; (ii) seismic-induced effects evaluated by means of the plastic mechanism analysis, as shown in row C2 of Fig. 4. The free-body distribution of forces depicted in Fig. 4-C2 assumes uniform yielding of diagonals (see Fig. 2(a)), thus resulting in small bending demand on the brace-intercepted beam.

3.1.3 Criterion 3

Differently from C2, the third criterion (C3) accounts for the potential activation of soft-storey mechanisms (see Fig. 2(b)), as follows:

- The design provisions for diagonals members are the same as C2, as well as the control of storey-to-storey variation of brace tension overstrength ratios.
- The brace-intercepted beam is designed for combined axial force, shear force and bending moment, considering the conditions (i) of C2 for gravity loads, while seismic-induced effects are evaluated by means of the plastic mechanism analysis in which V and inverted V bracings above and below the beam are alternatively disregarded, as shown in Fig. 4-C3. As it can be trivially recognized this assumption results in higher bending demand in the beam than the effects calculated for beams in C2.
- The seismic-induced effects on columns are evaluated by performing plastic mechanism analysis, in which both V and inverted V bracings above and below the beam are assumed to reach their ultimate resistance in tension and post-buckling strength in compression.

3.1.4 Criterion 4

The fourth design criterion (C4) is consistent with the rules provided by AISC-341-16, as summarized hereinafter using symbolism with EN1998-1:

- The diagonal members are designed to withstand both tension and compression forces evaluated by performing global elastic analysis on a TC model. The “expected” strengths correspond to $\gamma_{ov}N_{pl,br,i}$ for braces in tension and to $\gamma_{ov}\chi N_{pl,br,i}$ for those in post-buckling range.
- The geometrical slenderness KL/r (being K the effective length factor depending on boundary conditions, L the unsupported length of the element and r the radius of gyration) are not greater than 200, thus resulting in slightly relaxed requirement as respect to the corresponding rule given by EN1998-1.
- The required strengths of non-dissipative members (i.e. beams and columns) are evaluated by considering the most severe condition between: (i) seismic induced axial forces evaluated by mean of linear-elastic analysis and amplified by a unique overall overstrength factor Ω_o equal to 2; (ii) seismic-induced effects evaluated by performing a plastic analysis in which V and inverted V bracings above and below the beams are alternatively in pre- and post-buckling range, namely as follows:
  a) all diagonal members transfer their expected pre-buckling resistance $\gamma_{ov}\chi N_{pl,br,i}$;
  b) the tension diagonals exhibit their expected plastic strength $\gamma_{ov}N_{pl,br,i}$, while those under compression attain their residual resistance set equal to $0.3\gamma_{ov}\chi N_{pl,br,i}$ (where χ is the buckling reduction factor

defined according to EN 1993-1-1).

It is interesting to observe that, similarly to the loading pattern considered in C2, the condition b) leads to small design actions at the mid-length of the brace-intercepted beam. Differently from EN1998-1, the AISC 341 the post-buckling capacity implicitly depends on the brace slenderness (by mean of the buckling strength $\chi N_{pl,br,i}$), thus overcoming the EN1998-1 inconsistencies.

3.1.5 Criterion 5

The fifth criterion (C5) incorporates and combines remarks inferred by the discussion on the currently codified design provisions and remarks from literature outlined in the previous Sections, as follows:

- The diagonal members at the i-th storey verify $N_{b,br,Rd,i} \geq N_{Ed,br,i}$ where $N_{b,br,Rd,i}$ is the design buckling strength of brace cross-section and $N_{Ed,br,i}$ is calculated by performing a global elastic analysis with TC model.
- The brace normalized slenderness $\bar{\lambda}$ is not greater than 2.

The storey-to-storey distribution of brace overstrength is controlled as respect to the buckling resistance of braces, as follows

$$[(\Omega_{b,i}-\Omega_b)/\Omega_b]\leq 0.25 \quad (2)$$

where $\Omega_b = min(\Omega_{b,i}) = min(N_{b,br,Rd,i}/N_{Ed,br,i})$, $i \in [1,(n-1)]$ and n is the number of storeys, thus excluding the braces at the roof storeys (generally characterized by the largest overstrength due to the requirement on limitation of slenderness) to avoid oversizing of the diagonals at lower and intermediate storeys.

- The seismic-induced effects on non-dissipative members (i.e., beams and columns) are calculated by means of plastic mechanism analysis assuming the most severe scenario between: (i) both V and inverted V bracings above and below the beam transmit their expected ultimate tensile strength $N_{T,br,i}=1.1\gamma_{ov}N_{pl,br,i}$ and post-buckling resistance $N_{C,br,i}=0.3\gamma_{ov}\chi N_{pl,br,i}$ (which corresponds to the condition of uniform yielding, see Fig. 2(a)). (ii) the forces in V and inverted V bracings above and below the beam are alternatively disregarded (which can be associated to the condition of soft-storey plastic mechanism, see Fig. 2(b)).
- The columns belonging to the braced bays are designed considering the combined action of the axial force (which is the most severe from conditions (i) and (ii)) and uniform bending moment in the plan of the braced frame equal to the 20% of the plastic flexural resistance of the column cross section in accordance with CSA-S16.
- In addition, the brace-intercepted beam is designed to have flexural stiffness K_b at the intersection with diagonals not smaller than 0.2 times the vertical stiffness K_{br} of the braces. K_b is calculated as follows

$$K_b = 48\zeta \cdot \frac{E \cdot I_b}{L_b^3} \quad (3)$$

where E is the Young modulus of steel, I_b is the second moment of area of the beam cross-section, L_b is the beam length and ζ depends on the boundary condition; (ζ = 4 for fixed ends and ζ = 1 for pinned ends.

K_{br} is calculated as

$$K_{br} = 2 \cdot \frac{E \cdot A_{br}}{L_{br}} \cdot sin^2\alpha \quad (4)$$

Being A_{br} the area of diagonal cross-section, L_{br} the brace length and α the angle of the slope of the diagonals.

3.2 Investigated structures

The five design procedures described in the previous section were applied to design a set of residential steel building, shown in Fig. 5. Two different plan configurations are considered either with 3×3 or 5×5 spans with 3, 6 and 12 storeys. The location of the bracings per frame type is also shown in Fig. 5. The span length is equal to 7 m, while the interstorey height is equal to 3.50 m for the i-th storey and 4.00 m for the first level. Rigid diaphragm is assumed at each level. The structural design for gravity loads and the relevant safety verifications are carried out according to European codes (i.e., EN1990, EN1991-1-1, EN1993-1-1, EN1994-1-1). Both non-seismic and seismic loads are given in Table 1.

The same behaviour factor q = 4 is assumed for all examined cases, consistently to the value recommended by EN 1998-1 for X-CBFs. At damage limitation (DL) limit state the limit for interstorey drift ratios is set equal to 0.75% (i.e., ductile non-structural elements).

Class 1 cross sections according to EN 1993:1-1 are used for all diagonal members. In addition, the width-to-thickness limits provided by AISC 341 for high ductile members are adopted for bracings designed according to C4 (namely for AISC-compliant frames).

Tables 2-7 summarize the structural properties of all examined archetypes.

Table 1 Design loads

Non-seismic loads	
Permanent load	Roof: 5.20 kN/m^2 Intermediate: 5.20 kN/m^2
Live load	Roof: 2.00 kN/m^2 Intermediate: 2.00 kN/m^2
Snow	0.5 kN/m^2
Cladding and partition	1.00 kN/m^2
Seismic loads	
Reference peak ground acceleration a_{gR}	0.35g
Soil type	C
Spectral shape	Type 1

Table 2 Structural members obtained for 12-storey-5 braced bays frames

	C1			C2			C3			C4			C5		
Storey	Column	Beam	Brace	Column	Beam	Brace(d×t)	Column	Beam	Brace(d×t)	Column	Beam	Brace(d×t)	Column	Beam	Brace(d×t)
	S355	S355	S355	S355	S355	S355	S355	S355	S355	S355	S355	S355	S355	S355	S355
12	HEM400	HEB220	HEA120	HEA400	HEA220	139.7×5	HEA400	HEA260	121×6.3	HEA400	HEA220	114.3×6	HEA400	HEA260	121×5
11	HEM400	HEB280	HEB120	HEA400	HEA280	159×6.3	HEA400	HEB400	127×10	HEA400	HEB280	127×8	HEA400	HEB400	127×10
10	HEM400	HEB220	HEB120	HEA400	HEA220	177.8×8	HEA400	HEA260	168.3×8	HEA400	HEA220	139.7×10	HEA400	HEA260	159×8
9	HEM400	HEB260	HEB160	HEA400	HEA260	193.7×8	HEA400	HEB400	168.3×10	HEA400	HEB280	168.3×8	HEM400	HEB500	168.3×10
8	HEM400	HEB220	HEB160	HEB400	HEA220	193.7×10	HEB400	HEA260	219.1×8	HEM400	HEA220	168.3×10	HEM400	HEA260	193.7×8
7	HD400×463	HEB220	HEM120	HEB400	HEA240	219.1×10	HEB400	HEB400	219.1×10	HEM400	HEB280	168.3×12	HD400×463	HEB500	219.1×8
6	HD400×463	HEB260	HEM120	HEM400	HEA260	219.1×12	HEM400	HEA260	219.1×12	HEM400	HEA260	193.7×10	HD400×463	HEA300	219.1×8
5	HD400×463	HEB220	HEM120	HEM400	HEA240	219.1×12.5	HEM400	HEM400	219.1×12	HD400×463	HEB280	193.7×10	HD400×463	HEM400	219.1×10
4	HD400×463	HEB260	HEM140	HD400×463	HEA260	219.1×16	HD400×463	HEA300	219.1×12.5	HD400×463	HEA260	193.7×12	HD400×509	HEA300	219.1×10
3	HD400×463	HEB220	HEM140	HD400×463	HEA240	219.1×16	HD400×463	HEM400	219.1×12.5	HD400×463	HEB280	193.7×12	HD400×509	HEM500	219.1×10
2	HD400×463	HEB260	HEM140	HD400×463	HEA260	219.1×16	HD400×463	HEA300	219.1×12.5	HD400×463	HEA260	193.7×12.5	HD400×634	HEA300	219.1×10
1	HD400×463	HEB280	HEM160	HD400×463	HEA280	219.1×16	HD400×463	HEM400	219.1×16	HD400×509	HEB280	219.1×12	HD400×634	HEM500	219.1×12.5

Table 3 Structural members obtained for 12-storey-3 braced bays frames

	C1			C2			C3			C4			C5		
Storey	Column	Beam	Brace	Column	Beam	Brace(d×t)	Column	Beam	Brace(d×t)	Column	Beam	Brace(d×t)	Column	Beam	Brace(d×t)
	S355	S355	S355	S355	S355	S355	S355	S355	S355	S355	S355	S355	S355	S355	S355
12	HEB400	HEB220	HEA120	HEA400	HEA220	121×4	HEA400	HEA260	101.6×8	HEA400	HEA220	101.6×6	HEA400	HEA260	114.3×5
11	HEB400	HEB260	HEA120	HEA400	HEA240	159×5	HEA400	HEB400	114.3×12.5	HEA400	HEB280	114.3×10	HEA400	HEB400	114.3×10
10	HEB400	HEB220	HEB120	HEA400	HEA220	177.8×6.3	HEA400	HEA260	159×8	HEA400	HEA220	139.7×8	HEA400	HEA260	139.7×8
9	HEM400	HEB260	HEB140	HEA400	HEA240	193.7×8	HEA400	HEB400	168.3×8	HEA400	HEB280	159×8	HEM400	HEB400	177.8×6
8	HEM400	HEB220	HEB160	HEB400	HEA220	193.7×10	HEB400	HEA260	219.1×8	HEM400	HEA220	168.3×8	HEM400	HEA260	168.3×8
7	HEM400	HEB260	HEM120	HEB400	HEA240	219.1×10	HEB400	HEB400	219.1×10	HEM400	HEB280	168.3×10	HEM400	HEB450	193.7×8
6	HEM400	HEB260	HEM120	HEM400	HEA260	219.1×12	HEM400	HEA260	219.1×10	HEM400	HEA260	168.3×12	HD400×463	HEA300	193.7×8
5	HD400×463	HEB220	HEM120	HEM400	HEA240	219.1×12.5	HEM400	HEM400	219.1×12	HEM400	HEB280	168.3×12	HD400×463	HEM400	193.7×10
4	HD400×463	HEB260	HEM140	HD400×463	HEA260	219.1×12.5	HD400×463	HEA300	219.1×12.5	HD400×463	HEA260	193.7×10	HD400×463	HEA300	193.7×10
3	HD400×463	HEB220	HEM140	HD400×463	HEA240	219.1×12.5	HD400×463	HEM400	219.1×12.5	HD400×463	HEB280	193.7×10	HD400×463	HEM400	219.1×8
2	HD400×463	HEB280	HEM160	HD400×463	HEA260	219.1×16	HD400×463	HEA300	219.1×12.5	HD400×463	HEA260	193.7×12	HD400×551	HEA300	219.1×8
1	HD400×463	HEB280	HEM160	HD400×463	HEA240	219.1×16	HD400×463	HEM400	219.1×16	HD400×463	HEB280	219.1×10	HD400×551	HEM400	219.1×10

Table 4 Structural members obtained for 6-storey-5 braced bays frames

	C1			C2			C3			C4			C5		
Storey	Column	Beam	Brace	Column	Beam	Brace(d×t)	Column	Beam	Brace(d×t)	Column	Beam	Brace(d×t)	Column	Beam	Brace(d×t)
	S355	S355	S355	S355	S355	S355	S355	S355	S355	S355	S355	S355	S355	S355	S355
6	HEB300	HEB260	HEA120	HEA400	HEA220	159×5	HEA400	HEB220	159×5	HEA400	HEA220	127×8	HEA400	HEA220	139.7×8
5	HEB300	HEB340	HEB160	HEA400	HEA260	177.8×8	HEA400	HEB400	177.8×8	HEA400	HEA260	168.3×8	HEA400	HEM320	177.8×8
4	HEB360	HEB260	HEM120	HEA400	HEA220	193.7×10	HEA400	HEB220	193.7×10	HEA400	HEA240	177.8×10	HEM400	HEA260	219.1×8
3	HEB360	HEB340	HEM140	HEM400	HEA260	193.7×12	HEM400	HEB400	193.7×12	HEB400	HEA260	193.7×10	HEM400	HEM400	219.1×10
2	HEM400	HEB260	HEM140	HEM400	HEA220	193.7×12	HEM400	HEB220	219.1×12	HEM400	HEA240	193.7×12	HD400×463	HEB260	219.1×10
1	HEM400	HEB340	HEM160	HEM400	HEA260	219.1×12	HEM400	HEM400	219.1×12.5	HEM400	HEA260	219.1×10	HD400×463	HEM500	219.1×12

Table 5 Structural members obtained for 6-storey-3 braced bays frames

	C1			C2			C3			C4			C5		
Storey	Column	Beam	Brace	Column	Beam	Brace(d×t)	Column	Beam	Brace(d×t)	Column	Beam	Brace(d×t)	Column	Beam	Brace(d×t)
	S355	S355	S355	S355	S355	S355	S355	S355	S355	S355	S355	S355	S355	S355	S355
6	HEB300	HEB260	HEA120	HEA400	HEA220	159×5	HEA400	HEA220	101.6×4	HEA360	HEA220	127×8	HEA360	HEA220	139.7×6
5	HEB300	HEB300	HEB140	HEA400	HEA260	168.3×8	HEA400	HEB280	121×6.3	HEA360	HEA280	159×8	HEA360	HEM300	168.3×8
4	HEB360	HEB260	HEM120	HEA400	HEA220	193.7×10	HEA400	HEA220	139.7×6.3	HEA360	HEA220	168.3×10	HEM400	HEA240	193.7×8
3	HEB360	HEB300	HEM120	HEM400	HEA260	177.8×12.5	HEB400	HEB320	139.7×8	HEB400	HEA280	177.8×10	HEM400	HEM360	193.7×10
2	HEM400	HEB260	HEM140	HEM400	HEA220	193.7×12	HEB400	HEA220	159×8	HEM400	HEA240	177.8×10	HEM400	HEA300	193.7×12
1	HEM400	HEB300	HEM160	HEM400	HEA260	219.1×12	HEB400	HEB400	159×10	HEM400	HEA300	219.1×10	HD400×463	HEM500	219.1×12

Table 6 Structural members obtained for 3-storey-5 braced bays frames

	C1			C2			C3			C4			C5		
Storey	Column	Beam	Brace	Column	Beam	Brace(d×t)	Column	Beam	Brace(d×t)	Column	Beam	Brace(d×t)	Column	Beam	Brace(d×t)
	S355	S355	S355	S355	S355	S355	S355	S355	S355	S355	S355	S355	S355	S355	S355
3	HEB340	HEB400	HEB120	HEA300	HEB280	177.8×6	HEA400	HEB320	177.8×6	HEA360	HEB360	159×8	HEA400	HEB400	177.8×6
2	HEB340	HEB260	HEM120	HEA300	HEA220	193.7×8	HEA400	HEB220	193.7×10	HEA360	HEA240	168.3×12	HEA400	HEA260	193.7×8
1	HEB340	HEB400	HEM140	HEA300	HEB280	219.1×10	HEA400	HEM320	193.7×12	HEA360	HEB360	193.7×12	HEB400	HEM400	219.1×10

Table 7 Structural members obtained for 3-storey-3 braced bays frames

	C1			C2			C3			C4			C5		
Storey	Column	Beam	Brace	Column	Beam	Brace(d×t)	Column	Beam	Brace(d×t)	Column	Beam	Brace(d×t)	Column	Beam	Brace(d×t)
	S355	S355	S355	S355	S355	S355	S355	S355	S355	S355	S355	S355	S355	S355	S355
3	HEB340	HEB360	HEB120	HEA300	HEB280	159×6.3	HEA400	HEB300	159×6.3	HEA360	HEB360	139.7×8	HEA400	HEB360	159×5
2	HEB340	HEB220	HEB160	HEA300	HEA220	193.7×8	HEA400	HEA220	193.7×8	HEA360	HEA220	168.3×8	HEA400	HEA220	193.7×6.3
1	HEB340	HEB360	HEM120	HEA300	HEB280	219.1×8	HEA400	HEB400	193.7×10	HEA360	HEB360	168.3×12	HEA400	HEM320	193.7×8

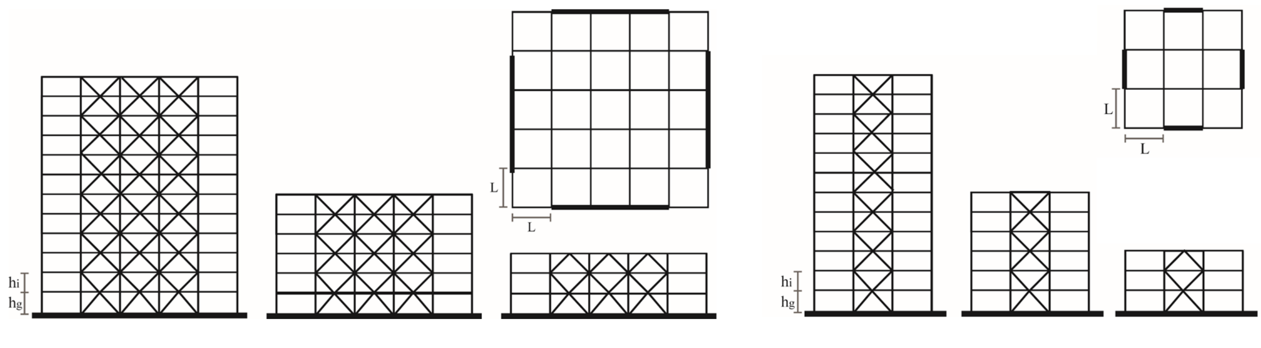

Fig. 5 Structural archetypes and analysed 2D frames

4. Seismic performance evaluation

4.1 Modelling assumptions

The numerical models of designed 2D frames are developed in Seismostruct; the main modelling assumptions (e.g., material, structural members, mass, second order effects) are consistent with those already used and validated against experimental results in previous studies carried out by the Authors (Costanzo *et al.* 2017a, b, 2019).

The structural members are modelled using the force-based (FB) distributed inelasticity elements (Spacone *et al.* 1996), accounting for distributed inelasticity through integration of material response over the cross section and integration of the section response along the length of the element. The cross-section response is simulated by the fibre approach, i.e., assigning a uniaxial stress-strain relationship at each fibre. The Menegotto-Pinto (Menegotto and Pinto 1973) hysteretic model is used to reproduce the steel behaviour.

The hysteretic behaviour of diagonal members is simulated by using the physical-theory model (PTM) as shown by D'Aniello *et al*. (2013, 2014). An initial camber is applied at the brace mid-length, calculated according to Dicleli and Calik (2008) and consistently with results by D'Aniello *et al*. (2013, 2014), showing that this approach is appropriate to simulate both the buckling and the hysteretic behaviour (thus including post-buckling range) of bracing elements. The numerical integration method used is based on the Gauss-Lobatto distribution (Abramowitz and Stegun 1964); 5 Gauss-Lobatto integration points (IP) are used.

The P–Δ effects are accounted for by using a "leaning column", namely by assigning the gravity loads that are not tributary to the examined planar frames to a fictitious column providing no stiffness and connected to the main frame using pinned rigid links

The diagonal members are assumed fully restrained in-plane, while the out-of-plane end condition at the gusset plate location is based on models developed by Hsiao *et al*. (2012). The size of the gusset plates is accounted for by means of rigid elements at whose tip an out-of-plane rotational spring is located to simulate the connection behaviour (see Fig. 6).

The hysteretic response of the spring at the diagonal end is characterized by a bilinear elastic-plastic symmetric response curve. The initial rotational stiffness is derived as follows

$$k_i = \frac{E}{L_{av}}\left(\frac{W_w \cdot t^3}{12}\right) \qquad (5)$$

where E is the young modulus of steel, W_w is the width of the Whitmore section (Whitmore 1952), t is the thickness of the gusset plate, and L_{av} is the average of L_1, L_2 and L_3 shown in Fig. 6. The post-yielding stiffness is defined as the 3% of the initial stiffness, while the flexural resistance of the gusset plate is estimated as follows

$$M_y = f_y \cdot W_{pl,w} \qquad (6)$$

being f_y the yielding strength of the steel and $W_{pl,w}$ the plastic modulus of the section of the plate at the Whitmore section.

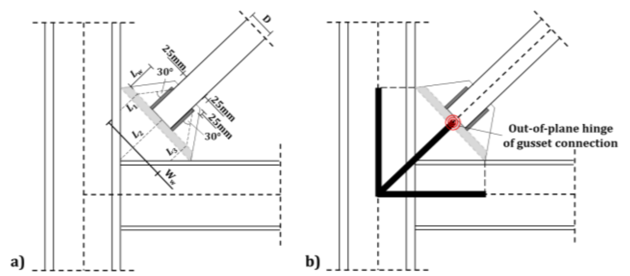

Fig. 6 Geometrical features of the designed gusset plate connections

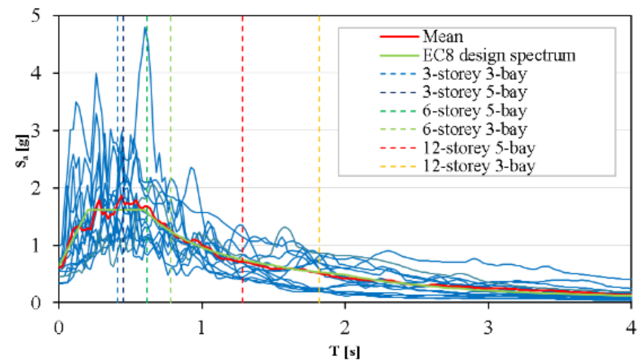

Fig. 7 Comparison between natural records and EN1998-1 design spectrum

4.2 Selected accelerograms

The nonlinear dynamic time-history analyses were performed by using a set of 14 natural earthquake acceleration records selected to match the EN1998-1 design spectrum (Fig.7). The relevant data are reported in Table 8.

4.3 Monitored parameters

Global and local performance parameters were selected and monitored to assess the seismic response of the examined structures for the three limit states Damage Limitation (DL), Severe Damage (SD) and Near Collapse (NC) as defined according to Eurocode 8, namely earthquakes with 95, 475 and 2475 years-return period are respectively associated.

The monitored response parameters are:

(i) Peak transient interstorey drift ratio (IDR), namely the ratio between the peak relative displacements at two consecutive floors and the corresponding interstorey height.

(ii) Brace ductility demand in tension and compression, given by the following ratio

$$\mu = \frac{d}{d_y} \qquad (7)$$

where d is the diagonal axial displacement and d_y the displacement at yielding.

To check the occurrence of fracture in diagonal members the ratio $\frac{d}{\mu_r \cdot d_y}$ was also monitored, where μ_{fr} is half time (conservatively assuming symmetric imposed cyclic displacement histories) the normalized deformation capacity prior fracture calculated according to the empirical formulation provided by Goggins *et al.* (2006).

The normalized unbalanced force occurring on the beam in post-buckling range, calculated as

$$\beta = \frac{U_F}{4M_{pl,b}/L_b} \qquad (8)$$

where, $U_F=(N_T-N_C)\cdot\sin\alpha$ is the force applied on the beam resulting from the vertical components of axial forces (N_T, N_C) transmitted by the diagonals, while the ratio $4M_{pl,b}/L_b$ represent the force corresponding to the formation of plastic hinge at the beam mid-span (being L_b the beam length and $M_{pl,b}$ the beam plastic capacity).

Table 8 Data of natural acceleration records

Earthquake	Date	Station Name	Station Country	Magnitude Mw	Fault mechanism
Alkion	24.02.1981	Xylokastro-O.T.E.	Greece	6.6	Normal
Montenegro	24.05.1979	Bar-Skupstina Opstine	Montenegro	6.2	Reverse
Izmit	13.09.1999	Yarimca (Eri)	Turkey	5.8	Strike-Slip
Izmit	13.09.1999	Usgs Golden Station Kor	Turkey	5.8	Strike-Slip
Faial	09.07.1998	Horta	Portugal	6.1	Strike-Slip
L'Aquila	06.04.2009	L'Aquila - V. Aterno - AquilaPark In	Italy	6.3	Normal
Aigion	15.06.1995	Aigio-OTE	Greece	6.5	Normal
Alkion	24.02.1981	Korinthos-OTE Building	Greece	6.6	Normal
Umbria-Marche	26.09.1997	Castelnuovo-Assisi	Italy	6.0	Normal
Izmit	17.08.1999	Heybeliada-Senatoryum	Turkey	7.4	Strike-Slip
Izmit	17.08.1999	Istanbul-Zeytinburnu	Turkey	7.4	Strike-Slip
Ishakli	03.02.2002	Afyon-Bayindirlik ve Iskan	Turkey	5.8	Normal
Olfus	29.05.2008	Ljosafoss-Hydroelectric Power	Iceland	6.3	Strike-Slip
Olfus	29.05.2008	Selfoss-City Hall	Iceland	6.3	Strike-Slip

The demand-to-capacity ratios in terms of both bending moment vs. plastic moment (M/M_{pl}) and axial force vs. buckling resistance (N/N_b) of the columns belonging to the braced bays were also monitored at both SD and NC limit states to evaluate the effect of the axial-force bending interaction when additional bending moments develops in the columns with the increase of seismic demand.

The results obtained from analyses are presented hereinafter, by showing the average demand obtained by the 14 considered records per response indicator.

4.4 Discussion of results

Figs. 8 and 9 report the average IDR obtained at each limit state for the examined low, medium and high-rise frames with 3 and 5 braced bays, respectively. The frames designed according to C1 and C2 exhibit the poorest performance characterized by cantilever-type displacement profile with larger demand concentrated at the upper storeys than the lower ones.

This behaviour is more pronounced for 12-storey cases, whose response is more affected by the higher modes of vibration and rocking-like behaviour. Such result confirms that the condition of storey-to-storey variation of brace tension overstrength ratios Ω as currently provided by EN1998-1 is not effective to ensure uniform distribution of plastic deformation along the building height. Slightly better performance can be recognized for frames designed according to the third criterion (C3), which leads to larger lateral stiffness due to the design of heavier beam profiles, as respect to the cases designed according to C1 and C2. Very poor response is recognized solely for 6-storey and 5 braced bays frame with high drift demand at the upper storeys.

Frames designed according to both C4 and C5 criteria show good seismic performance with satisfactory lateral stiffness, shear-like displacement profiles with sufficient uniform distribution of deformation along the building height.

The better response can be recognized for frames designed according to the design criteria C5 with IDR values lower than 0.75%, 1% and 2% frames at DL, SD and NC respectively, thus also satisfying the requirements for non-structural damage at DL limit state. Slightly larger displacements are solely recognized for the 12-storey with 5 braced bays case at DL, even lower than 1%.

The brace ductility demand μ (see Eq. (7)) is shown in Figs. 10 and 11 at each limit state for all the examined frames with 3 and 5 braced bays, respectively, while the damage pattern (i.e. the diagonals yielded under tension and buckled under compression) is graphically reported in Figs. 12 and 13, with reference to the three limit states. The μ profiles are basically consistent with the relevant displacement shapes. The frames designed according to C5 exhibit the largest energy dissipation capacity with almost all braces under tension in plastic range at SD limit state, while limited and well distributed damage is recognized under compression. Similar behaviour is shown for frames designed according to C4, with slightly larger deterioration of diagonals under compression.

The ratio $\frac{d}{\mu_{fr} \cdot d_y}$ is also shown in Fig. 14 to monitor the occurrence of fracture in diagonal members: fracture occurs at NC collapse limit state solely for 12-storey 3-braced bay case designed according to C2, even though both C2 an C4 compliant cases exhibit brace axial deformation under compression very close to the limit μ_{fr}.. The bracings belonging to frames designed according to C5 are far from fracture at each storey.

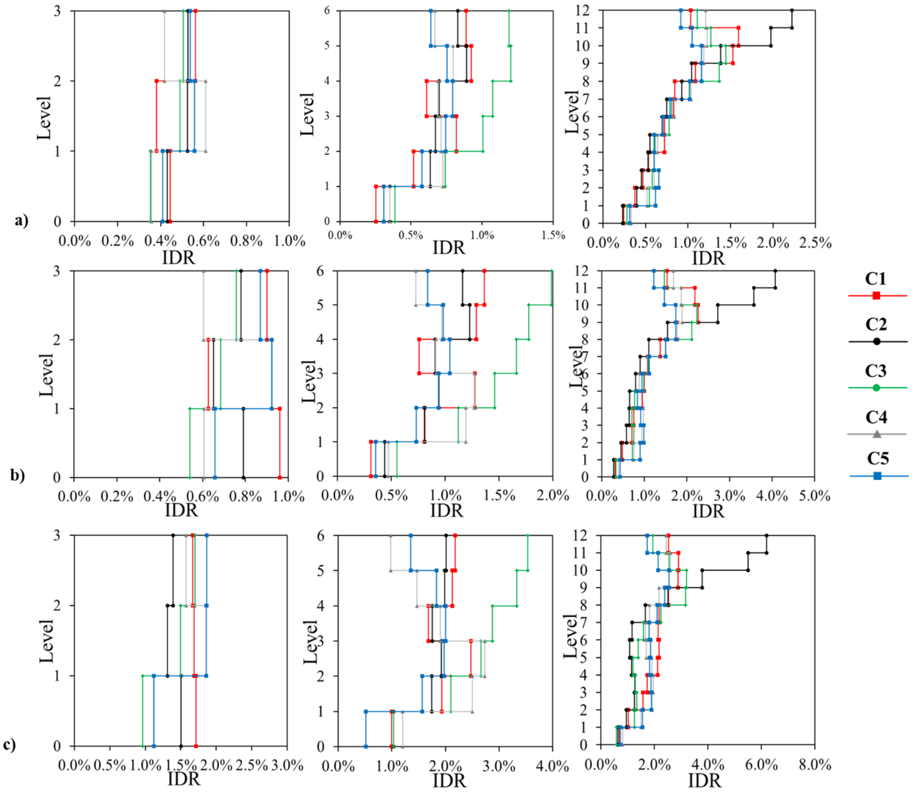

Fig. 8 Interstorey drift ratios (IDR) for 3, 6 and 12 storey frames with 3 braced bays at DL (a), SD (b) and NC (c) limit state

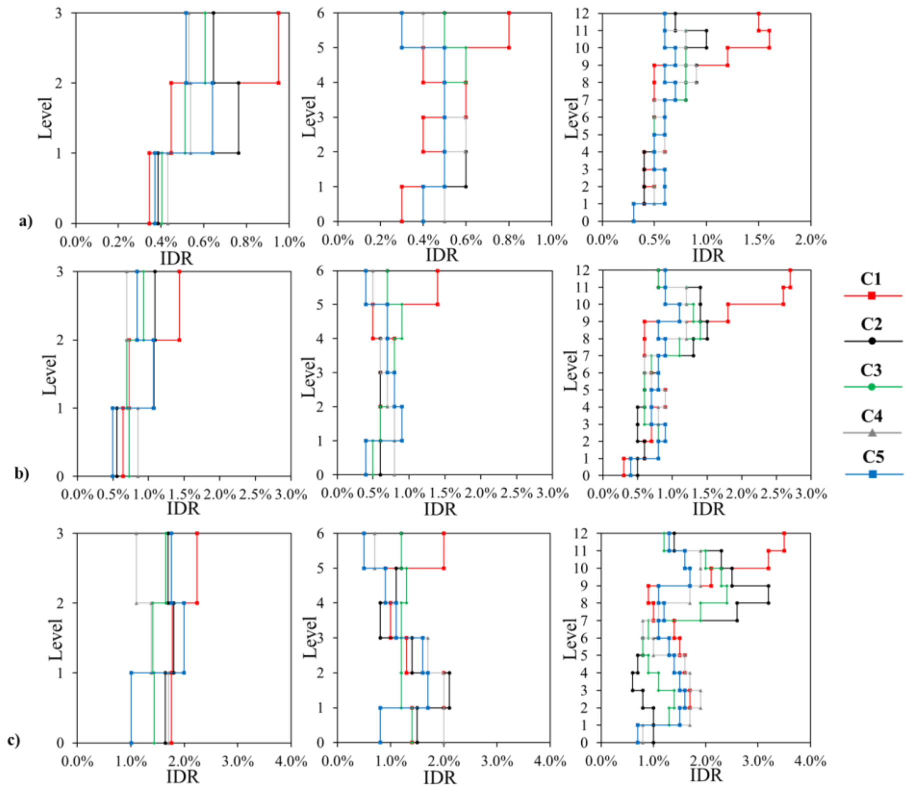

Fig. 9 Interstorey drift ratios (IDR) for 3, 6 and 12 storey frames with 5 braced bays at DL (a), SD (b) and NC (c) limit state

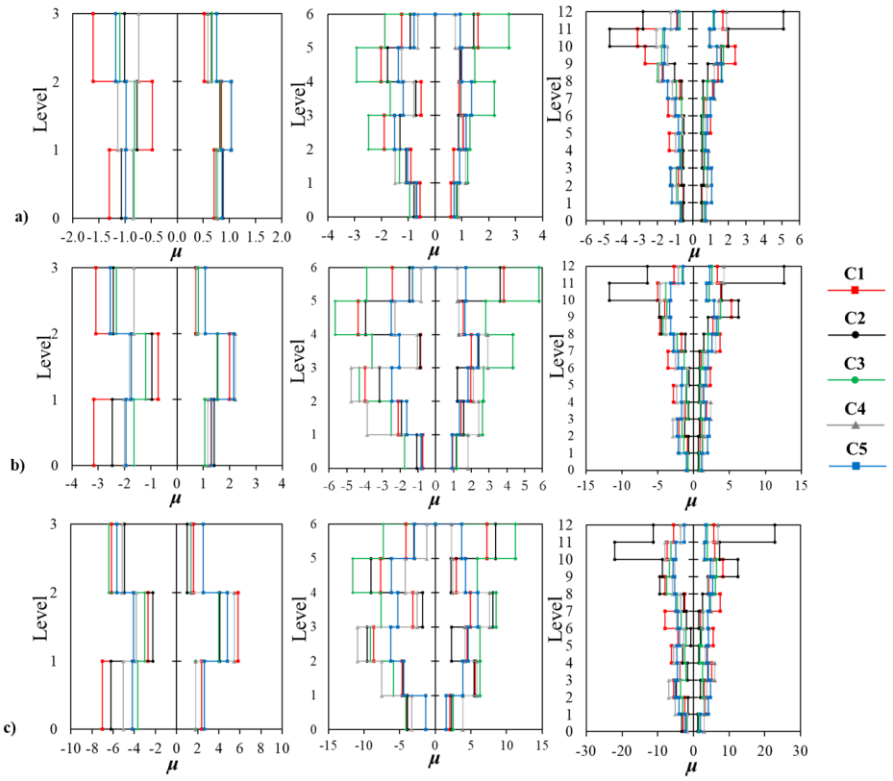

Fig. 10 Ductility demand of braces in tension and compression (μ) for 3, 6 and 12 storey frames with 3 braced bays at DL (a), SD (b) and NC (c) limit state

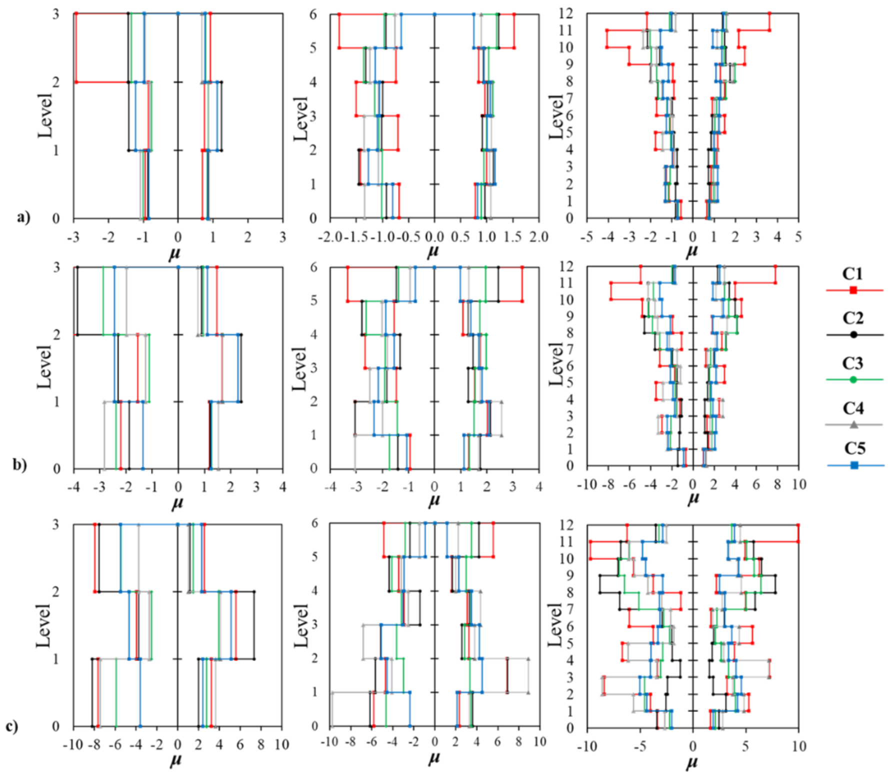

Fig. 11 Ductility demand of braces in tension and compression (μ) for 3, 6 and 12 storey frames with 5 braced bays at DL (a), SD (b) and NC (c) limit state

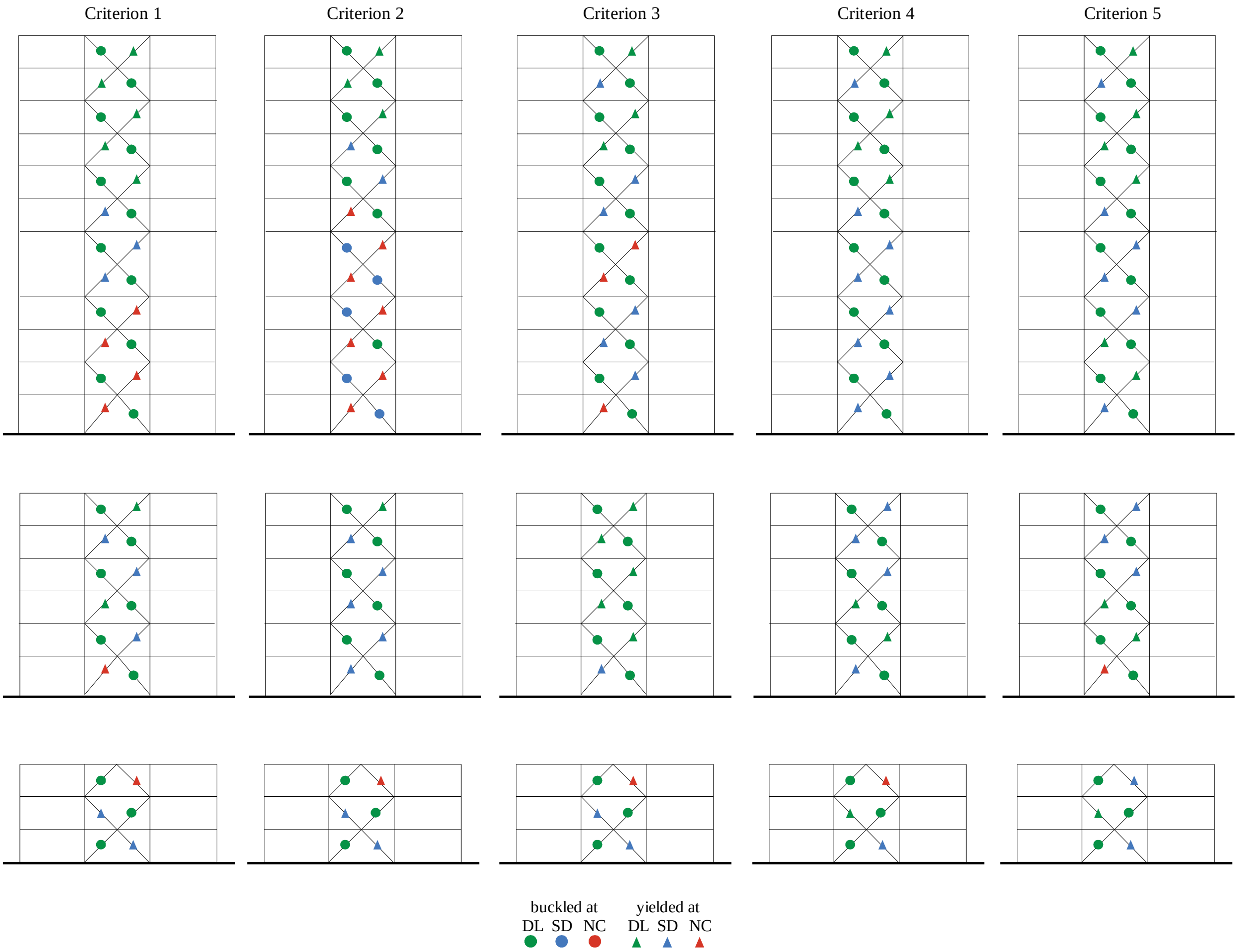

Fig. 12 Damage pattern (buckling/yielding) for braces in 3, 6 and 12 storey frames with 3 braced bays

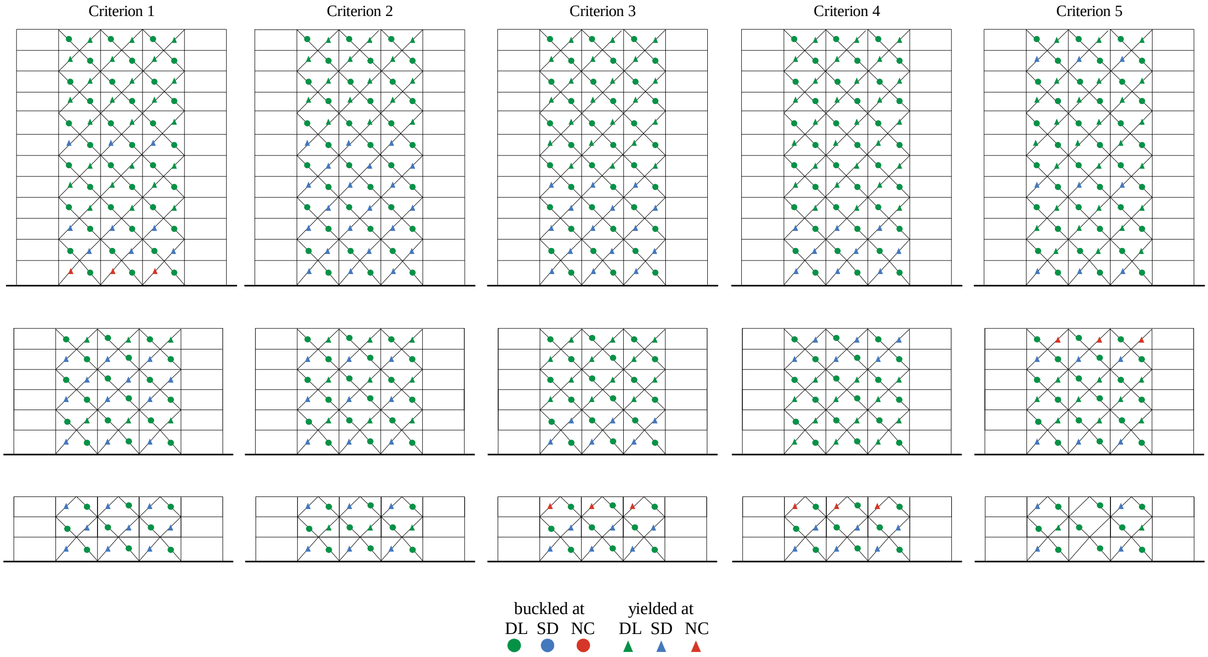

Fig. 13 Damage pattern (buckling/yielding) for braces in 3, 6 and 12 storey frames with 5 braced bays

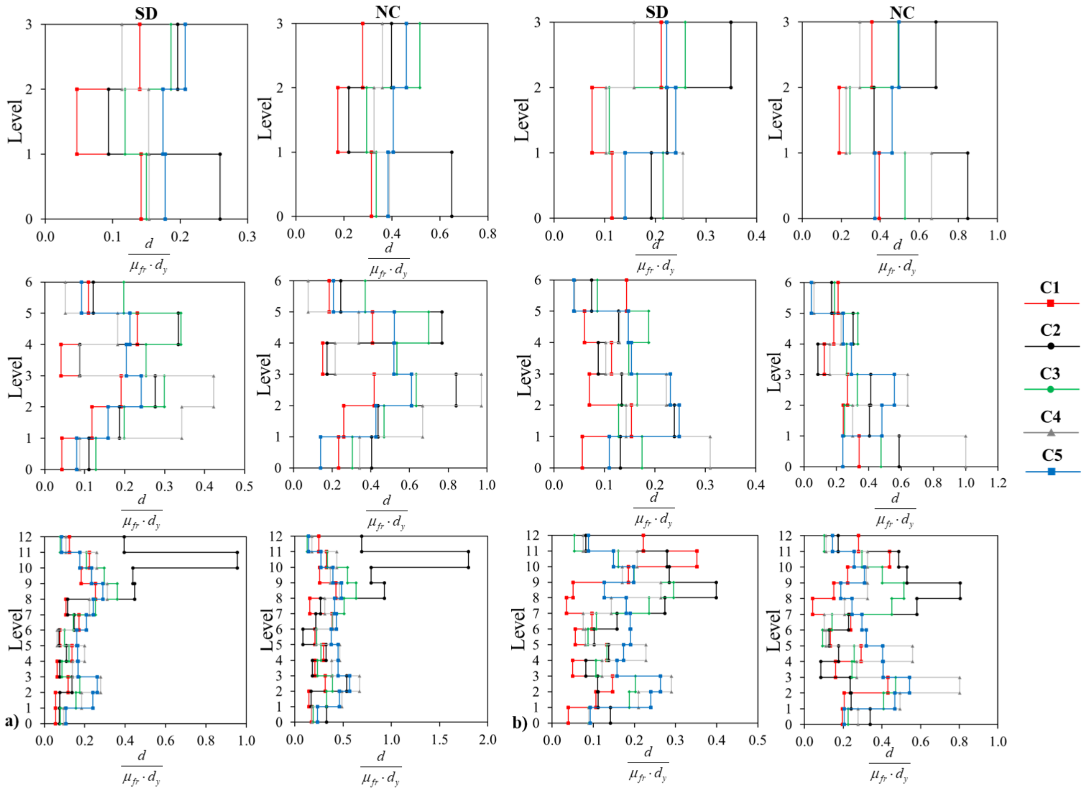

Fig. 14 Occurrence of fracture in diagonal members (μ_{fr}) for 3, 6 and 12 storey frames with (a) 3 braced bays and (b) 5 braced bays

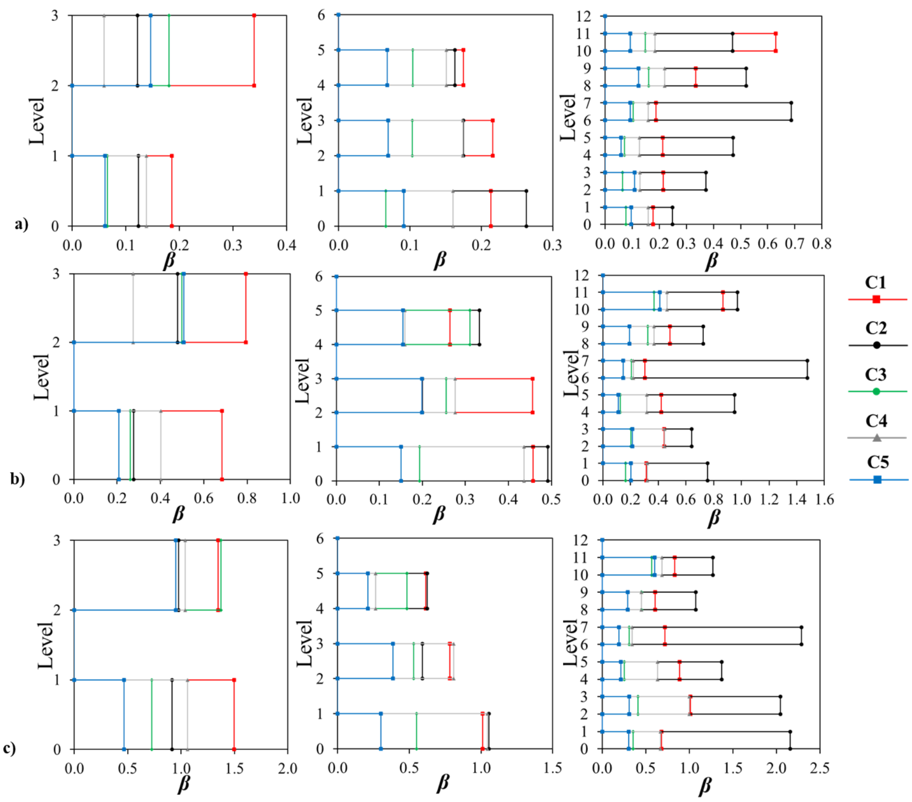

Fig. 15 Force (β) transferred by the braces to the beam for 3, 6 and 12 storey frames with 3 braced bays at DL (a), SD (b) and NC (c) limit state

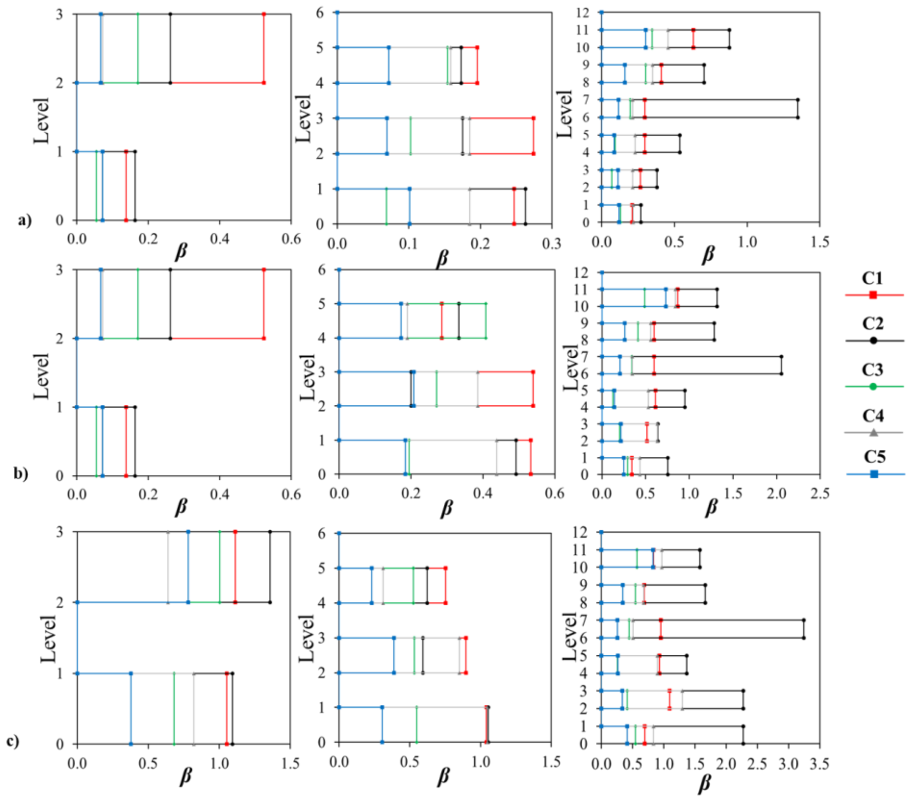

Fig. 16 Force (β) transferred by the braces to the beam for 3, 6 and 12 storey frames with 5 braced bays at DL (a), SD (b) and NC (c) limit state

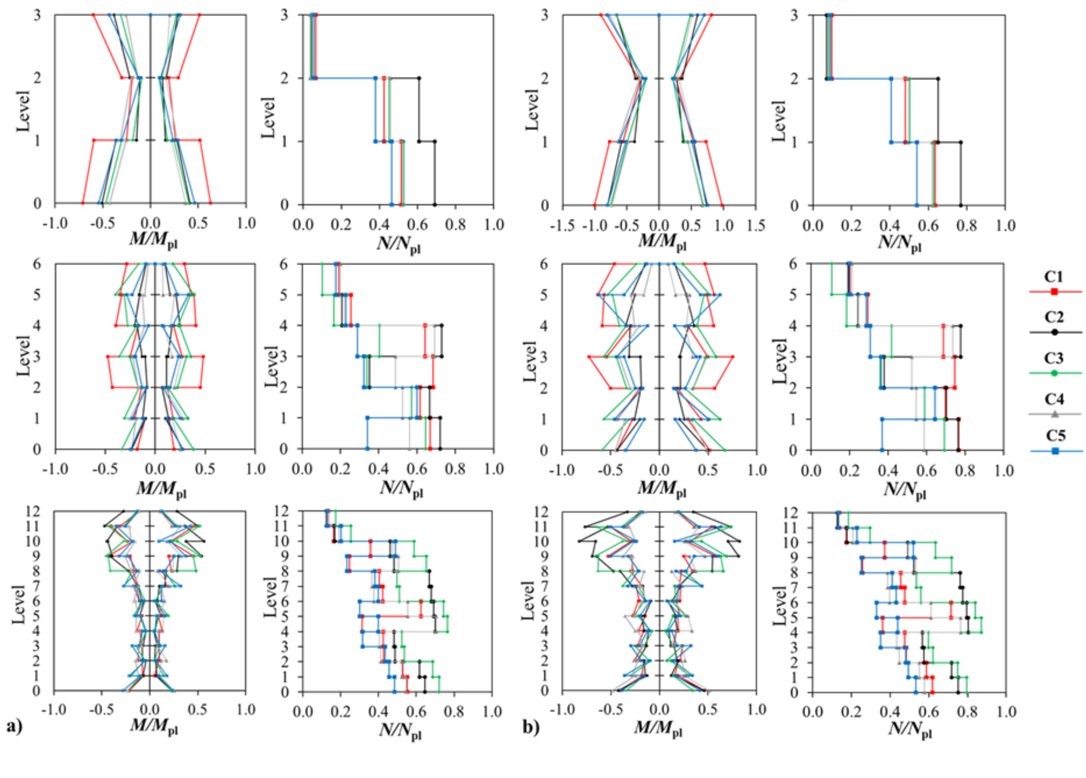

Fig. 17 Axial force (*N*) and bending moment (*M*) into the columns for 3, 6 and 12 storey frames with 3 braced bays at SD (a) and NC (b) limit state

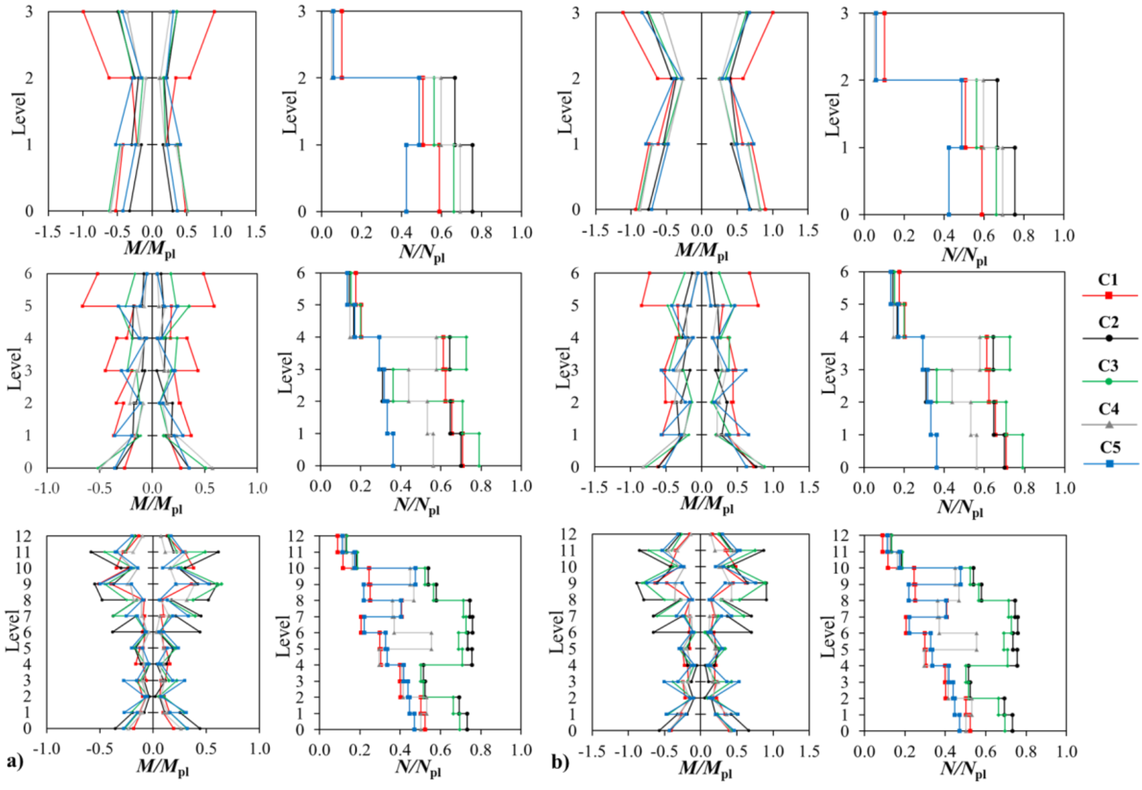

Fig. 18 Axial force (N) and bending moment (M) into the columns for 3, 6 and 12 storey frames with 5 braced bays at SD (a) and NC (b) limit state

The normalized vertical force (β) applied on the beam at the brace-intercepted section (see Eq. (8)) is depicted in Figs. 15 and 16 for all the examined frames with 3 and 5 braced bays, respectively. As expected, significantly smaller β values (i.e., corresponding to less engaged beams in bending) are recognized for the cases designed specifically accounting for potential occurrence of soft-storey mechanism (see Fig. 3(b)), which entails large required flexural beam strength (see Fig. 4-C3).

Thereby, no yielding occurs for frames designed according to both criteria C5 and C3. Conversely, the beam plastic capacity is exceeded ($\beta \geq 1$) for all low medium and high-rise frames designed according to both C1 and C2, while little plastic engagement is experienced solely in 12-storey frames designed according to C4. This result highlights that explicitly considering the activation of soft-storey mechanism (see Fig. 3(b)) is a key aspect to guarantee the effectiveness of hierarchy of resistances and ductile global plastic mechanism. The effect of axial force-bending moment interaction on the columns belonging to the braced bays can be observed from the plots in Figs. 17 and 18, where the maximum values of axial force and bending demand normalized to the relevant axial compression capacity (N_b) and plastic flexural strength (M_{pl}) are reported for the examined cases with three and five braced bays at both SD and NC limit states.

The results shown in Figs. 17-19 confirm that neglecting the bending moment into the columns at design stage is not conservative, as also recognized by Bosco *et al*. (2014). To clarify this aspect, Fig. 19 depicts the flexural capacity accounting for bending-compression axial force interaction (see Eq. (9)) for common European column profiles (HEB and HEM from 240 to 1000, and HD from 400x347 to 400x818) as a function of the normalized compression force N/N_b (being $N_b = \chi N_{pl}$) for three levels of bending demand ($M/M_{pl} = 0.2$; $M/M_{pl} = 0.5$; $M/M_{pl} = 0.8$) and different shape of the bending moment diagram, i.e., rectangular shape ($\Psi = 1$), triangular shape ($\Psi = 0$) and bi-triangular shape ($\Psi = -1$). For the sake of clarity, the bending-compression axial force
interaction is defined according to EN 1993-1-1 as

$$\Gamma = \frac{N_{Ed}}{\chi \cdot \dfrac{N_{pl}}{\gamma_{M1}}} + k_{yy} \cdot \frac{M_{Ed}}{\chi_{LT} \cdot \dfrac{M_{pl}}{\gamma_{M1}}} \tag{9}$$

where N_{Ed} is the compression force demand, N_{pl} is the plastic axial resistance of the profile; χ is the buckling reduction factor for uniform members in compression defined according to EN 1993-1-1; M_{Ed} is the bending demand; M_{pl} is the plastic bending resistance of the profile; χ_{LT} is the buckling reduction factor for uniform members in bending defined according to EN 1993-1-1; k_{yy} is the axial-bending interaction factor calculated according to Annex B of EN 1993-1-1.

As it can be observed, the columns could buckle for typical values of axial forces and bending moments obtained from non-linear analyses.

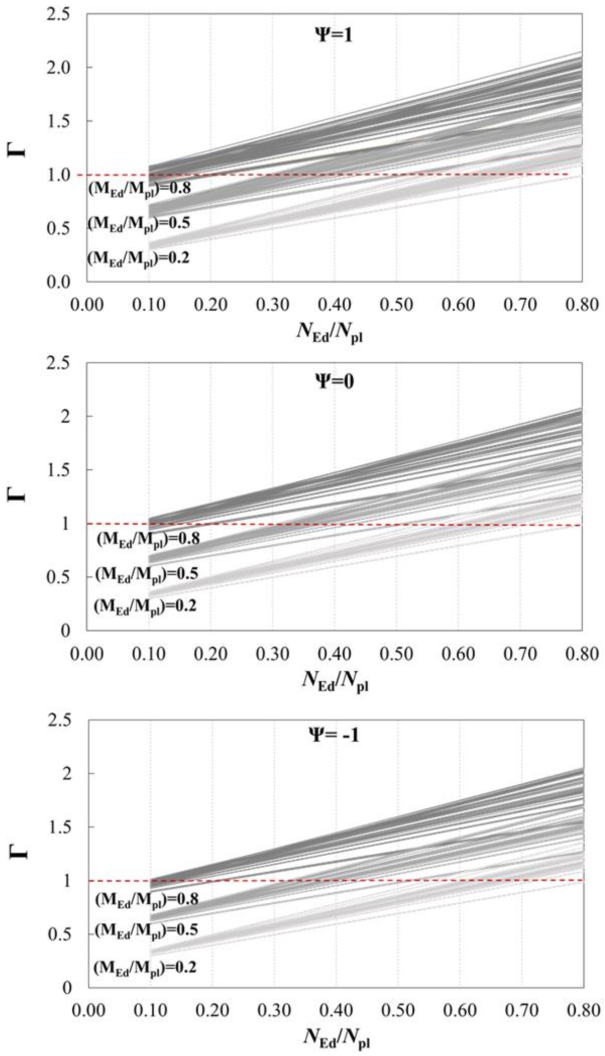

Fig. 19 Axial force and bending moment interaction in columns at different moment diagrams

The frames designed according to design criteria C5 exhibit values of axial force and bending moment smaller the 40% and the 50% of the relevant capacities, with triangular and bi-triangular moment diagram shape in the most of cases, at SD limit state. As it can be observed combining the outcomes of Figs. 17, 18 with Fig. 19 no column failure corresponds at SD and NC limit states. Conversely, the cases designed in compliance with C1, C2 and C3 show values of normalized axial force (0.7-0.8) and bending moment (0.5-0.6) exceeding the bending moment-compression force resistance Γ (see Fig. 19) in the most of cases even at SD limit states. Slightly better performance can be recognized for C4-compliant case with failure at SD solely recognized for three-storey frame. In addition, the combined axial force-bending moment demand significantly increases, and it exceeds the relevant capacity at NC limit stares.

5. Conclusions

Two-storey X-bracings are becoming very popular in European practice. However, such configuration is not properly addressed within the current EN1998-1. The research presented in this paper is addressed to revise the current Eurocode requirements and to propose potential amendments. In the light of remarks inferred by the discussion on current codes and existing literature, five different design criteria were discussed and numerically investigated.

The interpretation of numerical results inferred the following remarks:

- The frames designed according to the design criterion (C5) exhibit satisfactorily seismic response with adequate lateral strength and stiffness and shear-like displacement shape profiles with almost uniform plastic engagement of diagonals under tension and limited deterioration of those under compression along the building height.
- The check of storey-to-storey variation of brace tension overstrength required by current EN 1998-1 is not effective to ensure uniform distribution of plasticity and to avoid soft-storey mechanisms. Conversely, controlling the distribution of buckling overstrength rather than the tensile overstrength (see Eq. (2)) allows better controlling the sequence of braces buckling and the post-buckling distribution of drifts, thus forcing shear-like behaviour and avoiding damage concentration at any storey.
- The characterization of the loading pattern applied at the brace-intercepted beam has a key role in the design of two-storey concentrically braced frames. Indeed, applying the force distribution due to the contemporary occurrence of the ultimate tension and compression resistances of all braces (i.e., below and above each beam) may lead at underestimating the bending demand into the brace-intercepted beam.
- In order to get a conservative estimation of bending moments in the beam it is proposed to design the brace-intercepted beams against the most severe condition between (i) assuming both V and inverted V bracings above and below the beam attaining their ultimate resistance; (ii) assuming a soft-storey mechanism alternatively occurring below and above each beam.
- The interaction of compression axial force and bending moments acting on the columns belonging to the braced bays should be accounted for. The design rules in criterion C5 (which are consistent with CSA-16) for the axial force-bending moment interaction give satisfactory performance at EN1998-1 design limit state.

References

Abramowitz, M. and Stegun, I.A. (1964), Handbook of Mathematical Functions, National Bureau of Standards, Applied Math. Series

AISC Seismic Design Manual. 3rd Ed. Chicago, USA. American Institute of Steel Construction, Inc; 2018

American Institute of Steel Construction, Inc. (AISC). (2016), Seismic Provisions for Structural Steel Buildings. ANSI/AISC Standard 341-16. AISC, Chicago, Illinois

Astaneh-Asl, A., Cochran, M.L. and Sabelli, R. (2006), "Seismic Detailing of Gusset Plates for Special Concentrically Braced Frames", *Structural Steel Educational Council- Steel TIPS*.

Barbagallo, F., Bosco, M., Marino, E.M. and Rossi, P.P. (2019), "Achieving a more effective concentric braced frame by the double-stage yield BRB", *Eng. Struct.*, **186**, 484-497. https://doi.org/10.1016/j.engstruct.2019.02.028.

Bosco, M., Ghersi, A., Marino, E.M. and Rossi, P.P. (2014), "A capacity design procedure for columns of steel structures with diagonals braces", *Open Constr. Build. Technol. J.*, **8**, 196-207. DOI: 10.2174/1874836801408010196.

Bosco, M., Brandonisio, G., Marino, E.M., Mele, E. and De Luca, A. (2017), "Ω* method: An alternative to Eurocode 8 procedure for seismic design of X-CBFs", *J. Constr. Steel Res.*, **134,** 135-147. https://doi.org/10.1016/j.jcsr.2017.03.014.

Chen, C.H. and Mahin, S.A. (2012), "Performance based seismic demand assessment of concentrically braced steel frame buildings. PEER report 2012/103", Pacific Earthquake Engineering Research Center, Headquarters at University of California, Berkeley, California.

Costanzo, S., D'Aniello, M. and Landolfo, R. (2016), "Critical review of seismic design criteria for chevron concentrically braced frames: the role of the brace-intercepted beam", *Ing. Sismica: Int. J. Earthq. Eng.*, **33**(1-2), 72-89.

Costanzo, S., D'Aniello and M. and Landolfo, R. (2017a), "Seismic design criteria for chevron CBFs: European vs North American codes (part-1)", *J. Constr. Steel Res.*, **135**, 83-96. http://dx.doi.org/10.1016/j.jcsr.2017.04.018.

Costanzo, S., D'Aniello, M. and Landolfo, R. (2017b), "Seismic design criteria for chevron CBFs: Proposals for the next EC8 (part-2)", *J. Constr. Steel Res.*, **138**, 17-37. http://dx.doi.org/10.1016/j.jcsr.2017.06.028.

Costanzo, S. and Landolfo, R. (2017), "Concentrically braced frames: European vs. North American seismic design provisions", *Open Civil Eng. J.*, **11**(Suppl-1, M11), 453-463. DOI: 10.2174/1874149501711010453.

Costanzo, S., D'Aniello, M., Landolfo, R. and De Martino, A. (2018), "Critical discussion on seismic design criteria for cross concentrically braced frames", *Ing. Sismica: International J. Earthq. Eng.*, **35**(2), 23-36.

Costanzo, S., D'Aniello, M. and Landolfo, R. (2019), "Proposal of design rules for ductile X-CBFs in the framework of Eurocode 8", *Earthq. Eng. Struct D.*, **48**(1), 124-151. https://doi.org/10.1002/eqe.3128.

CSA. 2014. Design of Steel Structures, CSA-S16-14, Canadian Standards Association, Toronto, ON.

D'Aniello, M., Costanzo, S. and Landolfo, R. (2015), "The influence of beam stiffness on seismic response of chevron concentric bracings", *J. Constr. Steel Res.*, **112**, 305-324. https://doi.org/10.1016/j.jcsr.2015.05.021.

D'Aniello, M., La Manna Ambrosino, G., Portioli, F. and Landolfo, R. (2013), "Modelling aspects of the seismic response of steel concentric braced frames", *Steel Compos. Struct.*, **15**(5), 539-566. http://dx.doi.org/10.12989/scs.2013.15.5.539.

D'Aniello, M., La Manna Ambrosino, G., Portioli, F. and Landolfo, R. (2015b), "The influence of out-of-straightness imperfection in Physical-Theory models of bracing members on seismic performance assessment of concentric braced structures", *Struct. Des. Tall Spec. Build.*, **24**(3), 176-197. https://doi.org/10.1002/tal.1160.

Dicleli, M. and Calik, E.E. (2008), "Physical theory hysteretic model for steel braces", *J. Struct. Eng.- ASCE*, **134**(7), 1215-1228. ttps://doi.org/10.1061/(ASCE)0733-9445(2008)134:7(1215).

Elghazouli, A.Y. (2010), "Assessment of European seismic design procedures for steel framed structures", *Bull. Earthq. Eng.*, **8**, 65-89. https://doi.org/10.1007/s10518-009-9125-6.

EN 1990 (2001), Eurocode 0: Basis of structural design.

EN 1991-1-1 (2002), Eurocode 1: Actions on structures - Part 1-1: General actions -Densities, self-weight, imposed loads for buildings.

EN 1993:1-1 (2005), Eurocode 3: design of steel structures – part 1-1: general rules and rules for buildings.

EN 1994-1-1 (2004), Eurocode 4: Design of composite steel and concrete structures - Part 1.1: General rules and rules for buildings.

EN 1998-1-1. (2005), Eurocode 8: Design of structures for earthquake resistance – Part 1: General rules, seismic actions and rules for buildings.

Goggins, J.M., Broderick, B.M. and Elghazouli, A.Y. and Lucas, A.S. (2006), "Behaviour of tubular steel members under cyclic axial loading", *J. Constr. Steel Res.*, **62**(1-2), 121-31. https://doi.org/10.1016/j.jcsr.2005.04.012.

Hsiao, P., Lehman, D. and Roeder, C. (2012), "Improved analytical model for special concentrically braced frames", *J. Constr. Steel Res.*, **73**, 80-94. https://doi.org/10.1016/j.jcsr.2012.01.010.

Hsiao, P.C., Lehman, D.E. and Roeder, C.W. (2013), "Evaluation of the response modification coefficient and collapse potential of special concentrically braced frames", *Earthq. Eng. Struct. D.*, **42**, 1547-1564. doi:10.1002/ eqe.228.

Khatib, I.F., Mahin, S.A. and Pister, K.S. (1998), "Seismic behavior of concentrically braced steel frames", Report UCB/EERC-88/01. Earthquake Engineering Research Center, University of California, Berkeley, CA.

Longo, A., Montuori, R. and Piluso, V. (2008), "Failure mode control of X-braced frames under seismic actions", *J. Earth. Eng.*, **12**, 728-759. https://doi.org/10.1080/13632460701572955.

Longo, A., Montuori, R. and Piluso, V. (2015), "Seismic design of chevron braces coupled with MRF fail safe systems", *Earthq. Struct.*, **8**(5), 1215-1239. https://doi.org/10.12989/eas.2015.8.5.1215.

Longo, A., Montuori, R. and Piluso, V. (2016), "Moment frames – concentrically braced frames dual systems: analysis of different design criteria", *Struct. Infrastruct. Eng.*, **12**(1),122-141. https://doi.org/10.1080/15732479.2014.996164.

Marino, E.M. (2013), "A unified approach for the design of high ductility steel frames with concentric braces in the framework of Eurocode 8", *Earthq. Eng. Struct. D.*, **43**(1), 97-118. https://doi.org/10.1002/eqe.2334.

Menegotto, M. and Pinto, P.E. (1973), "Method of analysis for cyclically loaded R.C. plane frames including changes in geometry and non-elastic behaviour of elements under combined normal force and bending", *Symposium on the Resistance and Ultimate Deformability of Structures Acted on by Well Defined Repeated Loads.*

Metelli, G. (2013), "Theoretical and experimental study on the cyclic behaviour of X braced steel frames", *Eng. Struct.*, **46**, 763-773. https://doi.org/10.1016/j.engstruct.2012.08.021.

Seismosoft (2011), SeismoStruct - A computer program for static and dynamic nonlinear analysis of framed structures. Available from URL: www.seismosoft.com.

Shen, J., Wen, R., Akbas, B., Doran, B. and Uckan, E. (2014), "Seismic demand on brace-intersected beams in two-story X-braced frames", *Eng. Struct.*, **76**, 295-312. https://doi.org/10.1016/j.engstruct.2014.07.022.

Shen, J., Wen, R. and Akbas, B. (2015), "Mechanisms in Two-story X-braced Frames", *J. Constr. Steel Res.*, **106**, 258-277. https://doi.org/10.1016/j.jcsr.2014.12.014.

Shen, J., Seker, O., Akbas, B., Seker, P., Seyedbabak, M. and Faytarouni, M. (2017), "Seismic performance of concentrically braced frames with and without buckling", *Eng. Struct.*, **141**, 461-481. https://doi.org/10.1016/j.engstruct.2017.03.043.

Silva, A., Santos, L., Ribeiro, T. and Castro, J.M. (2018), "Improved seismic design of concentrically X-braced steel frames to Eurocode 8", *J. Earthq. Eng.*, DOI: 10.1080/13632469.2018.1528912.

Silva, A., Castro, J.M. and Monteiro, R. (2019), "Practical considerations on the design of concentrically-braced steel frames to Eurocode 8", *J. Constr. Steel Res.*, **158**, 71-85. https://doi.org/10.1016/j.jcsr.2019.03.011.

Spacone, E., Ciampi, V. and Filippou, F.C., (1996), "Mixed formulation of nonlinear beam finite element", *Comput. Struct.,* **58**(1), 71-83. https://doi.org/10.1016/0045-7949(95)00103-N.

Tremblay, R. and Tirca, L. (2003), "Behavior and design of multi-story zipper concentrically braced steel frames for the mitigation of soft-story response", *Proceedings of the conference on behaviour of steel structures in seismic areas*.

Uriz, P. and Mahin, S.A. (2008), "Toward earthquake-resistant design of concentrically braced steel-frame structures". PEER rep no. 2008/08 Pacific Earthquake Engineering Research Centre, College of Engineering, Univ. of California, Berkley.

Whitmore, R. (1952), "Experimental Investigation of Stresses in Gusset Plates", University of Tennessee, Tech. Rep. No. 16

Wijesundara, K.K., Nascimbene, R. and Rassati, G.A. (2018), "Evaluation of the seismic performance of suspended zipper column concentrically braced steel frames", *J. Constr. Steel Res.*, **150**, 452-461. https://doi.org/10.1016/j.jcsr.2018.09.003.

Yoo, J.H., Roeder, C.W. and Lehman, D.E. (2009), "Simulated behavior of multi-story X-braced frames", *Eng. Struct*., **31**(1), 182-197. https://doi.org/10.1016/j.engstruct.2008.07.019.

CC